Development 140, 1100-1110 (2013) doi:10.1242/dev.088989

The *tiptop/teashirt* genes regulate cell differentiation and renal physiology in *Drosophila*

Barry Denholm[1,*,‡], Nan Hu[1,*], Teddy Fauquier[2], Xavier Caubit[2], Laurent Fasano[2] and Helen Skaer[1,‡]

SUMMARY

The physiological activities of organs are underpinned by an interplay between the distinct cell types they contain. However, little is known about the genetic control of patterned cell differentiation during organ development. We show that the conserved Teashirt transcription factors are decisive for the differentiation of a subset of secretory cells, stellate cells, in *Drosophila melanogaster* renal tubules. Teashirt controls the expression of the water channel Drip, the chloride conductance channel CLC-a and the Leukokinin receptor (LKR), all of which characterise differentiated stellate cells and are required for primary urine production and responsiveness to diuretic stimuli. Teashirt also controls a dramatic transformation in cell morphology, from cuboidal to the eponymous stellate shape, during metamorphosis. *teashirt* interacts with *cut*, which encodes a transcription factor that underlies the differentiation of the primary, principal secretory cells, establishing a reciprocal negative-feedback loop that ensures the full differentiation of both cell types. Loss of *teashirt* leads to ineffective urine production, failure of homeostasis and premature lethality. Stellate cell-specific expression of the *teashirt* paralogue *tiptop*, which is not normally expressed in larval or adult stellate cells, almost completely rescues *teashirt* loss of expression from stellate cells. We demonstrate conservation in the expression of the family of *tiptop/teashirt* genes in lower insects and establish conservation in the targets of Teashirt transcription factors in mouse embryonic kidney.

KEY WORDS: Cell differentiation, *Drosophila*, Kidney, Malpighian tubule, Organogenesis, Tiptop/Teashirt

INTRODUCTION

Organs are assemblies of differentiated cells, arranged into distinct configurations that allow them to carry out specialised functions. Specific tasks carried out by a particular organ are emergent properties that result from the coordinated interplay of the different specialised cell types they contain. Although we have extensive understanding of the physiological activities of organs at multiple levels, we know far less about the developmental mechanisms and genetic networks that bring about physiological maturation. For example, how are physiologically distinct cell types, which differ in gene expression, shape, location and function, established during organogenesis? These are important and fundamental questions, as these processes ultimately underpin integrated function for all organs. Here, we investigate the developmental genetic networks that establish secretory function in the *Drosophila melanogaster* renal tubule.

The role of the excretory system of an animal is to remove harmful substances from the body and to regulate ionic, acid-base and fluid balance. In insects, the renal or Malpighian tubules (MpTs) – a set of simple epithelial tubes – carry out these activities. Studies of renal tubule physiology have provided insight into the mechanisms underlying the clearance of toxins and regulation of urine production and modification (Beyenbach et al., 2010; Dow and Davies, 2001; Dow and Davies, 2003; Maddrell, 1981; Wessing and Eichelberg, 1978). Primary urine is secreted by main segment cells, driven by ion transport across the epithelium (Fig. 1). In *Drosophila* two physiologically distinctive cell types drive this process: principal cells (PCs or Type I cells), and stellate cells (SCs or Type II cells). PCs transport potassium ions, establishing a favourable electrochemical gradient that allows chloride ion movement through channels in SCs; water follows by osmosis facilitated by aquaporin water channels also in SCs (Fig. 1B) (Kaufmann et al., 2005; O'Donnell et al., 1998). The volume of urine production is regulated by internal physiology and environmental conditions through haemolymph-borne hormonal signals (Coast et al., 2001; Maddrell et al., 1991; Terhzaz et al., 1999). For example, PCs are activated by both cGMP- and cAMP-mediated pathways (Cabrero et al., 2002; Johnson et al., 2005; Kean et al., 2002), whereas in SCs leucokinin acts on its receptor (LKR), which elevates the chloride conductance of SCs (Fig. 1B) (reviewed by Beyenbach et al., 2010).

The developmental origins of PCs and Type II cells differ. PCs derive from epithelial primordia that bud out from the embryonic hindgut. Type II cells originate from mesenchymal cells that integrate into the tubule epithelium during mid-embryogenesis, differentiating as SCs in the secretory region and as bar cells in the initial and transitional segments (Denholm et al., 2003) (Fig. 1A,B). SCs become spaced in a regular pattern between PCs and can be distinguished by their smaller nuclear size. *teashirt* (*tsh*), which encodes a zinc-finger transcription factor, is expressed in SCs as they integrate and is an early marker that distinguishes them from the PCs. We therefore reasoned that *tsh* might regulate SC differentiation. Previous reports indicate that the *tsh* paralogue *tiptop* (*tio*) is also expressed in embryonic fly MpTs (Laugier et al., 2005) and that a *tio/tsh* orthologue is expressed in the developing MpTs of the beetle *Tribolium castaneum* (Shippy et al., 2008), further suggesting that these genes have important conserved roles in the development and/or function of insect MpTs.

[1]Department of Zoology, Downing Street, Cambridge CB2 3EJ, UK. [2]Aix-Marseille Université, CNRS, IBDML UMR7288, 13288, Marseille, France.

*These authors contributed equally to this work
‡Authors for correspondence (bjd24@cam.ac.uk; hs17@cam.ac.uk)

Accepted 20 December 2012

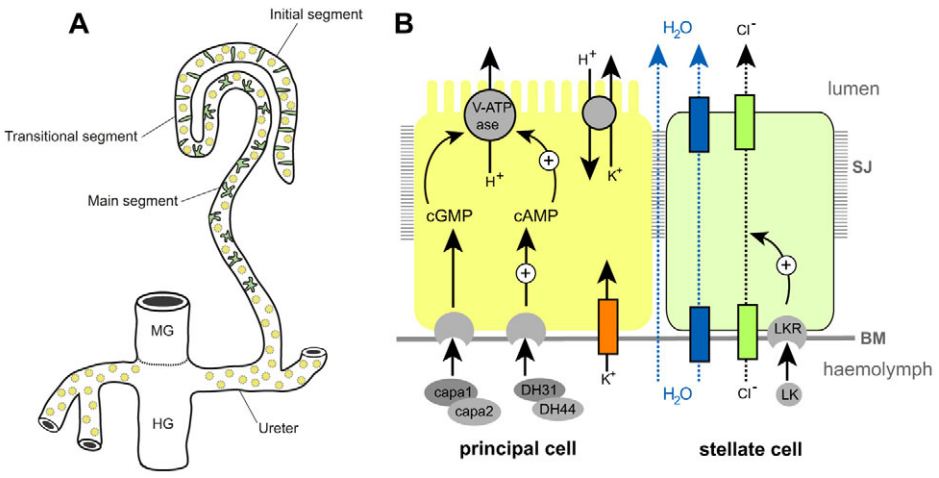

Fig. 1. *Drosophila* Malpighian tubules. (**A**) The four MpTs consist of initial, transitional and main segments, and a ureter. Stellate cells (SCs, green) are interspersed with principal cells (PCs, yellow) in the initial and transitional segments (where they are bar shaped), and throughout the secretory region of the main segment (where they are stellate). (**B**) The major physiological activities carried out by PCs (yellow) and SCs (green). Ion transport is driven by a H^+-transporting vacuolar-ATPase (V-ATPase) on the luminal membrane of PCs, which, coupled with a cation/H^+ antiporter, transports potassium ions into the lumen. Chloride ions move down an electrochemical gradient through chloride channels in SCs. Water (blue arrows) follows by osmosis through water channels in SCs and paracellular routes. Capability peptides 1/2 (Capa) and diuretic hormone 31/44 (DH) stimulate urine production through cGMP and cAMP pathways in PCs (Cabrero et al., 2002; Coast et al., 2001; Johnson et al., 2005; Kean et al., 2002). BM, basement membrane; LK, leucokinin; LKR, leucokinin receptor; SJ, septate junction.

Drosophila tsh and *tio* are paralogous genes that encode zinc-finger transcription factors (Laugier et al., 2005). The gene pair is present in the genomes of all *Drosophila* species sequenced to date (Clark et al., 2007) but only as a single gene in other insects (including the closely related Dipterans *Anopheles gambiae* and *Aedes aegypti*), suggesting a recent duplication event. Comparison of the genes among insects reveals that *tio* is the more ancestral gene, with *tsh* possessing more derived characteristics (Datta et al., 2011a; Datta et al., 2011b; Herke et al., 2005; Santos et al., 2010; Shippy et al., 2008). In the embryo, *tsh* promotes trunk segmental identities (Fasano et al., 1991) and contributes to the patterning of other tissues, such as the salivary glands and midgut (Henderson et al., 1999; Mathies et al., 1994). Later, *tsh* contributes to the specification and patterning of adult appendages, including the leg, wing and eye (Bessa et al., 2009; Bessa and Casares, 2005; Bessa et al., 2002; Erkner et al., 1999; Singh et al., 2004; Singh et al., 2002; Soanes et al., 2001; Sun et al., 1995; Wu and Cohen, 2000; Wu and Cohen, 2002). In many tissues, *tio* acts redundantly with *tsh* so that flies lacking *tio* function are viable without obvious phenotypes.

Vertebrate *teashirt* family genes (Tshz) have been identified in humans, mice, chick, zebrafish and frog (Santos et al., 2010), where they act to pattern multiple tissues during embryogenesis (Caubit et al., 2008; Caubit et al., 2010; Erickson et al., 2011; Faralli et al., 2011; Koebernick et al., 2006). Human TSHZ genes have proven or putative roles as disease loci, including juvenile angiofibroma, congenital aural atresia, congenital pelvi-ureteric junction obstruction, and breast and prostate cancers (Caubit et al., 2008; Feenstra et al., 2011; Jenkins et al., 2010; Schick et al., 2011; Yamamoto et al., 2011), although their precise roles in normal development and disease have not been established. Mouse Tshz genes are able to rescue the loss of trunk identity in *Drosophila melanogaster* (Manfroid et al., 2004), suggesting conservation over a wide evolutionary range.

Here, we characterise the genetic network that underpins physiological maturation in the MpTs. We find that *tsh* is a principal component of the SC differentiation hierarchy, controlling SC shape and the expression of genes required for terminal physiological differentiation. We show how *tsh* activity in SCs translates into integrated organ function and how this, in turn, influences the physiology of the whole animal, providing comprehensive insight into the function of Tsh-family transcription factors at multiple biological levels. We provide evidence that *tio/tsh* function in MpTs is conserved between insects separated in evolution by over 360 million years and, by extending our work to identify *Tshz3* targets in the mouse kidney, reveal that some downstream components of the *teashirt* genetic network are shared between invertebrates and vertebrates.

MATERIALS AND METHODS

Fly stocks

Flies were cultured on standard media at 18°C or 25°C with ectopic expression at 25ºC or 29ºC. The following stocks were used: UAS-*tsh*-RNAi P{TRiP.JF02856}attP2 (Bloomington 28022); c724-Gal4 (Sözen et al., 1997); tsh^{8}; tio^{S21}; *Df(2L)tt*, UAS-CD8-GFP; LKR protein trap [FlyTrap YD0927 (Quiñones-Coello et al., 2007)]; CtB-Gal4 (Sudarsan et al., 2002); UAS-*tsh* [(Datta et al., 2009), original source A. Courey, UCLA, CA, USA]. Embryos were collected on apple juice-agar plates.

Generation of *tsh tio* double mutant

We generated a 5 kb deficiency in *tio* (tio^{S21}) (supplementary material Fig. S1) by imprecise excision of the P-element *tio-Gal4*^{A4} (Tang and Sun, 2002). We then mobilised a w^+ P-element in a tio^{S21} mutant background and screened for potential new insertions at the *tsh* locus using the characteristic 'graded-eye' phenotype (dark red fading to white along the anterior-posterior axis). P-element rescue confirmed that one insertion (tsh^{GE4}) was in *tsh* (supplementary material Fig. S1). However, this line was homozygous viable with normal *tsh* expression. We therefore created an imprecise excision of this line to create a deficiency in *tsh*. Breakpoints were mapped by PCR from single homozygous mutant embryos using paired primers at ~10 kb intervals across the entire *tsh-tio* locus. This compound deficiency, *Df(2L)tt* (supplementary material Fig. S1), removes seven protein-coding and one non-protein-coding genes between *tsh* and

tio. We confirmed that protein expression is abolished in *Df(2L)tt* by staining for anti-Tsh and anti-Tio (supplementary material Fig. S1).

Tubule secretion assay

Secretion assays were performed as described previously (Dow et al., 1994) at 23-25°C using 3- to 5-day-old adult flies. cAMP and LK (Sigma) were added at a final concentration of 1 mM and 100 μm, respectively, after ~30 and 60 minutes.

Lethal phase analysis

c724-Gal4 >tsh-RNAi (n=900) or control (c724-Gal4 alone, n=600) embryos were collected in batches of 100 and maintained at 25°C. Surviving animals were counted as: first instar hatchlings, pupae and eclosing adults.

Fly weight measurements

To measure wet-body weight, flies were anaesthetized with CO_2, transferred to Eppendorf tubes on ice and weighed on a Mettler Toledo precision balance in triplicate. For dry-body weight, flies were sacrificed by freezing for 20 minutes and dried in a 50°C oven containing silica crystals for ~24 hours and weighed again.

In situ hybridisation

In situ hybridisation was carried out using digoxigenin-labelled RNA probes to embryonic and adult tissues as described previously (Denholm et al., 2005). To make the probes, we used RE60324 (*Drip*) and RE62514 (*ClC-a*). Embryos were dehydrated and mounted in Durcupan; adult tubules were mounted directly in 50% glycerol.

Immunohistochemistry

Antibody staining was carried out under standard conditions. Larval and adult tubules were dissected in ice-cold PBS and fixed (4% paraformaldehyde/PBS) on ice for up to 30 minutes, followed by 20 minutes at room temperature. The following antibodies were used: rabbit anti-Tsh (1:3000, S. Cohen, IMCB, Singapore), rat anti-Tio (1:500) (Laugier et al., 2005), mouse anti-Cut (1:200, DSHB), goat anti-GFP (1:500, Abcam) and mouse anti-Discs large (1:1000, DSHB). Appropriate biotinylated secondary antibodies were used with the Vector Elite ABC Kit (Vector Laboratories, CA, USA) for DAB staining. FITC- or Cy3-conjugated secondary antibodies were used for fluorescent labelling. When required, streptavidin-conjugated FITC/Cy3 amplification was used. TOTO3 (1:100, Molecular Probes) and DAPI (1:1000, Molecular Probes) were used to stain DNA and Alexa Fluor 488/568-conjugated phalloidin (Molecular Probes) to detect actin. Tissue was mounted in Vectashield (Vector Laboratories) and viewed on a Leica SP5 confocal microscope. Post-acquisition processing was performed using ImageJ and Adobe Photoshop, and final figures were assembled in Adobe Illustrator.

Mouse ureters were fixed in 4% paraformaldehyde/PBS. Immunostaining was performed on 16 μm cryosections, blocked in 10% normal donkey serum, 1% ice-cold water fish skin gelatin and 0.1% Triton X-100, prior to primary antibody incubation (overnight at 4°C, in PBS containing 0.05% Triton X-100, 1% normal donkey serum, 1% cold water fish skin gelatin and 1% DMSO) and rinsed before application of the secondary antibody. Primary antibodies used were mouse anti-smooth muscle α actin (SMaA, 1A4, Sigma; 1:1000) and rabbit anti-Aquaporin1 (AQP1, Millipore; 1:1000). Secondary antibodies used were DyLight488 and DyLight 633 (Jackson ImmunoResearch; 1:750). Sections were mounted in Prolong Gold (Invitrogen) and imaged with 25× oil immersion (NA 0.8) objectives using a confocal microscope (Zeiss LSM780). Sixteen-bit images were acquired sequentially for each channel to avoid bleed-through between DAPI, DyLight488 and DyLight633. Images were analysed using ImageJ.

3D reconstruction of SCs

High-resolution images of adult SC were made (z-slice of 200 nm). Three-dimensional surface rendering was carried out using Amira software with the surfacegen function. Surface area and volumes were calculated by tracing cell outlines for each z-slice, followed by reconstruction, surface smoothing (20 iterations with a lambda value of 0.9) and calculation of surface area and volume using Amira.

Affymetrix analysis

Total RNA was isolated from ureters using TRIsure Reagent (Bioline) according to manufacturer's instructions. The integrity of RNA was assessed using an Agilent 2100 Bioanalyzer (Agilent Technologies) and RNA concentration determined using a NanoDrop ND-1000 spectrophotometer (NanoDrop, Rockland, DE). cRNAs for hybridisation to Affymetrix arrays were prepared from 100 ng total RNA using the wild-type expression kit Affymetrix (Affymetrix, Santa Clara, CA 95051). Labelled-cRNA was fragmented and hybridised to mouse gene 1.0 ST arrays (Affymetrix) following manufacturer's protocols. Three independent RNA preparations from the two different conditions (wild type and mutant, embryonic stage E14.5) were processed and hybridised on Mouse Gene Arrays.

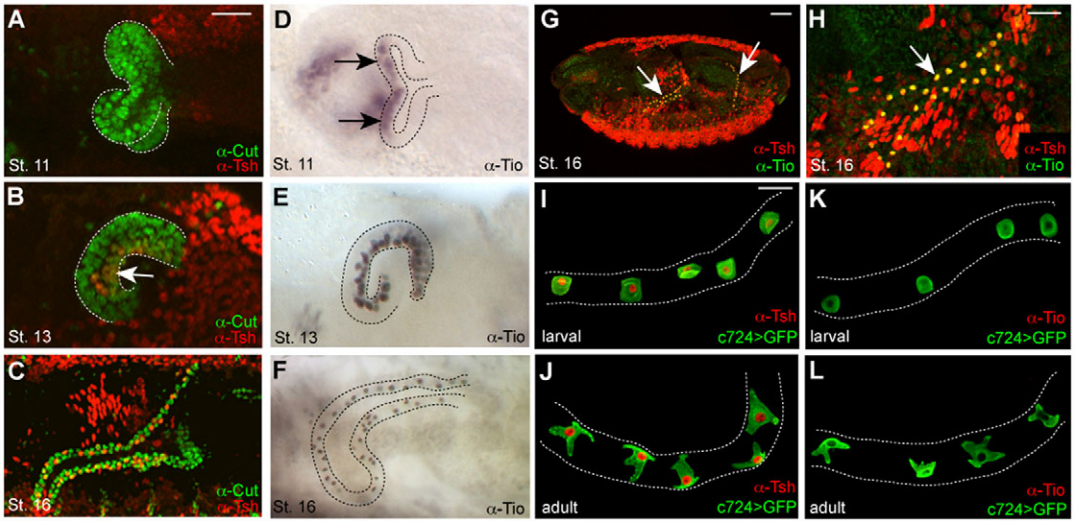

Fig. 2. Tsh and Tio expression in *Drosophila* tubules. (**A-F**) Tsh (red, A-C) and Tio (black, D-F) expression in embryonic MpTs. Tsh is first detected in SCs at stage 13 (B, arrow) and maintained throughout embryogenesis. Tio is first detected in PCs from stage 11 (D, arrows) and in SCs from stage 13 (E). By stage 16, Tio expression levels in SCs are high but diminished in PCs (F). (**G**,**H**) Low- (G) and high- (H) magnification views of stage 16 embryo showing Tsh (red) and Tio (green, overlap appears yellow) co-expression in SCs (arrows). (**I-L**) Tsh (red; I,J) and Tio (red; K,L) expression in larval (third instar; I,K) and adult (J,L) MpTs. Tsh but not Tio is expressed in larval and adult SCs. PCs are marked with anti-Cut (green, A-C) and SCs with c724>CD8GFP (green, I-L). Tubule outline is marked with broken lines. Scale bars: 50 μm in A-F; 50 μm in G,H; 30 μm in I-L.

RESULTS

Teashirt and Tiptop expression in *Drosophila melanogaster* Malpighian tubules

Tsh expression is first detected at low levels in a subpopulation of tubule cells at embryonic stage 13 (Fig. 2A,B). Based on their position on the posterior-facing side of the tubule (Denholm et al., 2003), we identify these cells as SCs. Tsh expression increases so that by stage 16, high levels are found in the entire SC population (Fig. 2C), which persists in larval and adult SCs (Fig. 2I,J). Tsh is not expressed in PCs at any stage (Fig. 2A-C,I,J). Expression of the *tsh* paralogue *tio* is found in a subset of PCs at stages 11 to 13 (Fig. 2D,E). Tio is first detected in SCs cells at stage 13 (Fig. 2E), when its expression in PCs begins to fade. By stage 16, Tio is restricted to SCs (Fig. 2F), overlapping completely with Tsh (Fig. 2G,H). Both genes are expressed in the initial, transitional and secretory region of the main segment and therefore encompass both SCs and bar-shaped cells. *tio* but not *tsh* is expressed in the distal-most tubule cell known as the tip cell (data not shown). These dynamic patterns of *tsh* and *tio* expression are in line with previous observations, where mutually exclusive patterns at early embryonic stages give way to co-expression at later stages (Laugier et al., 2005). In contrast to *tsh*, *tio* is not expressed in third instar larval or adult tubule cells (Fig. 2K,L). The expression of *tio/tsh* in Malpighian tubules implies an important function for these genes during tubule development. Furthermore, the maintenance of *tsh* expression in SCs through larval and adult life points to a function for *tsh* at later stages.

tsh and *tio* mutants lack morphological phenotypes in the embryo

We analysed *tsh* and *tio* single mutants, and *tsh tio* double mutants (using a novel deficiency we have generated; supplementary material Fig. S1) but found no morphological defects in embryonic tubules. Using a *tsh*-independent SC marker (G447.2-Gal4) (Georgias et al., 1997), we found that the normal number of SCs was specified and integrated into the tubules, intercalating between PCs with normal spacing (supplementary material Fig. S2A-D; see rare SC clustering in supplementary material Fig. S2D). The lack of penetrant morphological defects in the tubules led us to explore roles for *tio/tsh* in cell differentiation and tissue physiology.

tsh is required in SCs for organ function

tio is not expressed in larval and adult tubules (Fig. 2K,L), and *tio*-null mutants are viable and fertile (Laugier et al., 2005). We therefore focussed on the function of *tsh*. Because *tsh* mutants die as embryos (due to extra-renal defects) (Fasano et al., 1991), we used RNAi to knock down *tsh* in SCs cells using the *tsh*-GAL4, c724 (Sözen et al., 1997), which reflects a subset of *tsh* expression, including SCs from late embryonic stages throughout life (c724-GAL4>UAS-*tsh*RNAi, termed *tsh* knockdown). Anti-Tsh staining of adult tubules reveals complete knock down using this approach (supplementary material Fig. S3).

We compared tubule secretion in control and *tsh* knockdown tubules using an established *in vitro* assay (Dow et al., 1994; Ramsay, 1954) that measured: (1) basal secretory rates and (2) secretory rates after the addition of cAMP, an agonist that stimulates cation transport through secretory PCs, and (3) after further addition of leucokinin, an agonist that stimulates chloride flux through SCs (Fig. 1B; Fig. 3A). Basal secretory rates were significantly lower for *tsh* knockdown tubules than for wild type [peak secretion rates of 0.21±0.03 (s.e.m.) nl min^{-1}, n=10 versus 0.48±0.06 nl min^{-1}, n=9]. Addition of cAMP increased secretory rates in knockdown tubules; however, peak rates were significantly lower than wild type [0.38±0.04 (s.e.m.) nl min^{-1} versus 0.69±0.05 nl min^{-1}]. By contrast, leucokinin in addition to cAMP, which doubled secretory rate in wild-type tubules, had no further stimulatory effect in

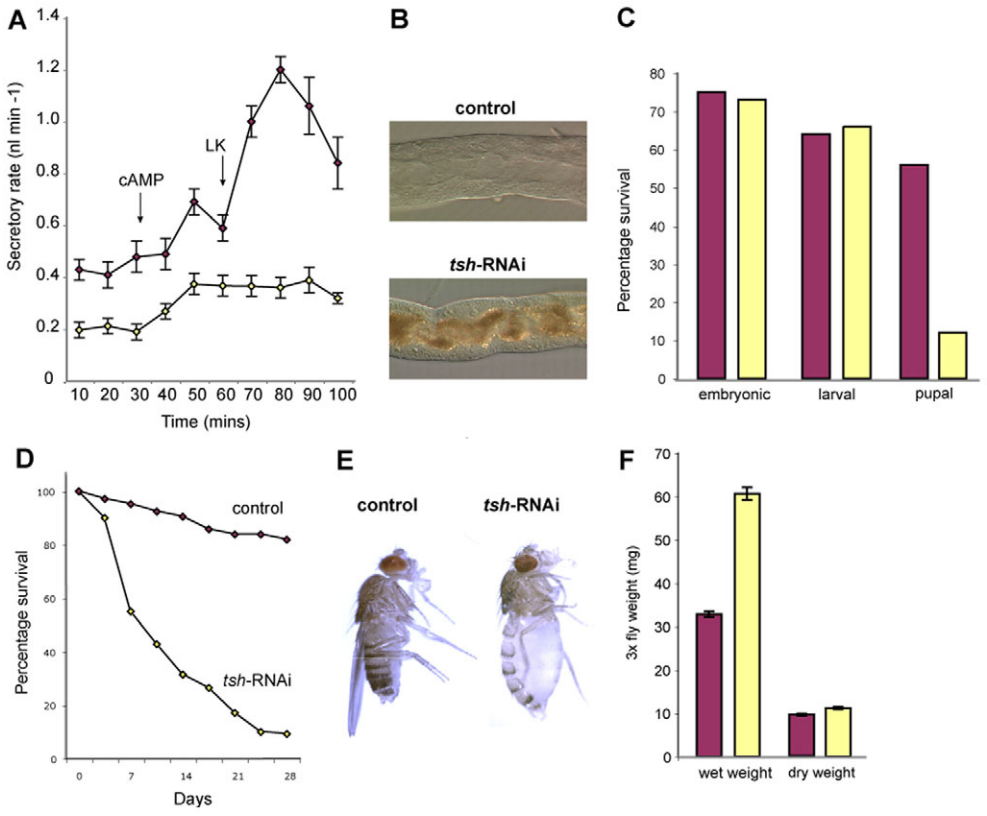

Fig. 3. Disrupted organ function and animal physiology in *tsh* knockdown flies. (**A**) Secretory rates (nl min^{-1}) in control (purple) and *tsh* knockdown (yellow) MpTs. Cyclic adenosine monophosphate (cAMP) and Leucokinin (LK) were added at ~30 and 60 minutes, respectively (arrows). Basal secretion rates are lower, and the response to LK is abolished in *tsh* knockdown tubules. (**B**) Uric acid crystals accumulate in the MpT lumen in the *tsh* knockdown. (**C**) Survival rates of control (purple, n=600) and *tsh* knockdown (yellow, n=900, nine replicates) animals from embryonic to pupal stages. The main lethal phase in *tsh* knockdown occurs during pupation. (**D**) Survival rates for control (purple, n=105) and *tsh* knockdown (yellow, n=140) adults. (**E**) Control (left) and *tsh* knockdown (right) 1-week-old adults. *tsh* knockdown adults have grossly distended abdomens. (**F**) Wet and dry weight measurements (mg; three flies/measurement) for adults: control (purple, n=13); *tsh* knockdown (yellow, n=26). Data are for females (equivalent results for males not shown).

knockdown tubules, with peak secretory rates remaining at 0.39±0.05 (s.e.m.) nl min^{-1} compared with 1.2±0.05 nl min^{-1} for wild-type (Fig. 3A). Compromised secretion for *tsh* knockdown tubules in intact animals is also suggested by the accumulation of high levels of luminal uric acid crystals that would normally be flushed away by urine flow (Fig. 3B). These data show that fluid secretion – a direct measure of tubule function – is significantly reduced in *tsh* knockdown tubules. We conclude that *tsh* activity in SCs is essential for the effective secretion of primary urine by MpTs.

tsh is required in SCs for full viability

To determine whether *tsh* knockdown in SCs affected whole-animal physiology, we compared viability between *tsh* knockdown and control (c724-Gal4 alone) flies. Embryonic and larval viability (number of eggs hatching and of larvae reaching pupation) is comparable for *tsh* knockdown and controls (73% versus 75% hatch and 66% versus 64% reach pupation, n=900 and 600, respectively). By contrast, only 12% of *tsh* knockdown animals emerge as adults compared with 56% of controls (Fig. 3C) and adult survival is strongly reduced (Fig. 3D). These data indicate that *tsh* in SCs is required for full viability during pupal and adult stages. As c724, although SC specific for tubules, is active in other tissues, such as the wing hinge (Soanes and Bell, 1999; Soanes et al., 2001), we cannot exclude the possibility that *tsh* knockdown elsewhere contributes to reduced viability.

tsh activity in SCs is required for normal fluid balance

Strikingly, *tsh* knockdown adults develop grossly distended abdomens within a few days of eclosion (Fig. 3E), a phenotype symptomatic of excess food intake (Al-Anzi et al., 2010), build up of internal gas or excess haemolymph volume, resulting from defective osmoregulation. We confirmed that the abdominal bloating was due to fluid retention in two ways. First, pricking submerged flies led to abdominal deflation without gas bubbles (data not shown). Second, wet weight measurements reveal that *tsh* knockdown adults are approximately twice as heavy as control flies, whereas dry weight measurements are equivalent, eliminating excess food intake as a cause of bloating (Fig. 3F). Together, these data show that *tsh* activity is required in SCs for normal organ function, which in turn is essential for fluid homeostasis.

Tsh regulates multiple features of the SC phenotype

Regulation of terminal gene expression

Next, we explored the role of *tsh* in SCs at the cellular level. We dismissed the simple hypothesis that a reduction in SC numbers caused the physiological defects in *tsh* knockdown flies; on average, each adult anterior tubule contained 34±1.5 (s.e.m.) c724-positive cells (n=12) and each posterior tubule contained 20±1 (n=10), compared with 33±1 (n=7) in each anterior and 20±1 (n=6) in each posterior tubule in wild type. Furthermore, the spacing of SCs in knockdown tubules was indistinguishable from wild type (Fig. 4A,B).

As *tsh* encodes a transcription factor, it could regulate the expression of genes that define SCs. We chose three candidates known to be highly expressed and/or to have well-defined activities in SCs [*Leucokinin receptor* (*Lkr*) (Radford et al., 2002); *Chloride channel-a* (*ClC-a*) (Wang et al., 2004); and the aquaporin water channel (*Drip*) (Kaufmann et al., 2005)] (Fig. 1B). We compared expression in wild-type versus *tsh* knockdown adult tubules by *in situ* hybridisation (for *Lkr*, *ClC-a* and *Drip*) and immunostaining a protein-trap line (for LKR; http://flytrap.med.yale.edu/) (Quiñones-Coello et al., 2007). In agreement with previous reports, *Lkr*, *Drip* and *ClC-a* are expressed in adult SCs (Fig. 4C,E,G) (Kaufmann et al., 2005; Radford et al., 2002; Wang et al., 2004). By contrast, *Lkr*, *Drip* and *ClC-a* expression were completely abolished on *tsh* knockdown in SCs (Fig. 4D,F,H). Thus, *tsh* plays a decisive role in SC differentiation, regulating the expression of terminal genes that are crucial for their physiological role. Failure of SC maturation will severely compromise hormone-induced fluxes of chloride ions and water and is likely to underlie the low basal secretory rates and defective diuretic response of tubules after *tsh* knockdown (Fig. 3A).

ClC-a is highly expressed in late embryonic SCs (Fig. 4I). To determine whether *ClC-a* is controlled by *tsh* at this stage, we

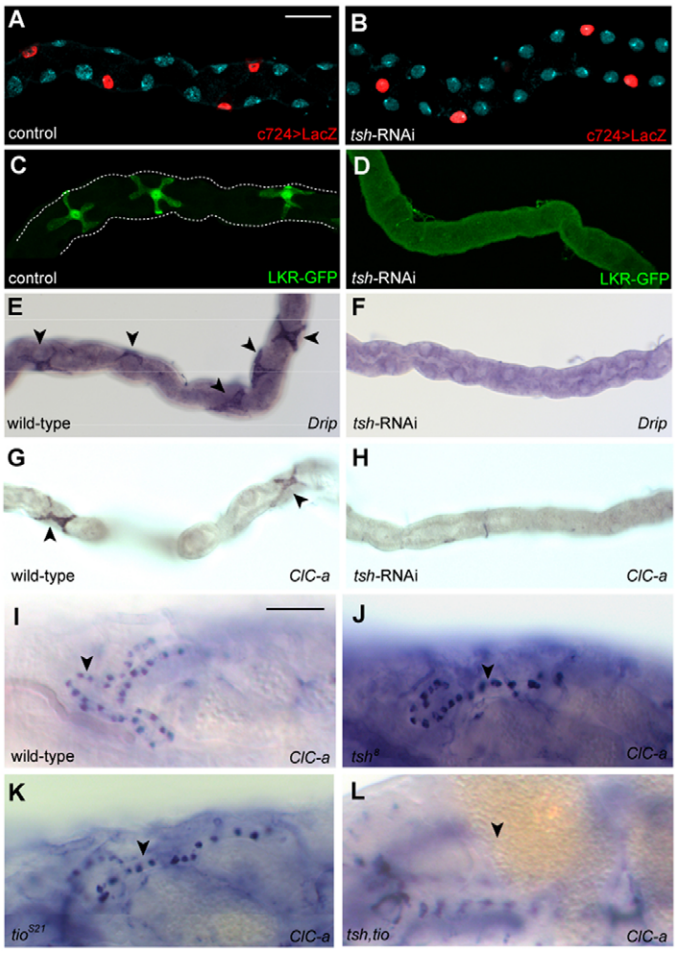

Fig. 4. *tsh* regulates terminal differentiation gene expression. (**A**,**B**) SC number and spacing is normal in control (A) and *tsh* knockdown (B) adult MpTs. SCs marked with c724>UAS-n*lacZ* (red), tubules counterstained for DNA (blue). (**C-H**) *tsh* regulates SC gene expression in MpTs. Adult MpTs from control or wild-type (C,E,G), or *tsh* knockdown (D,F,H) animals. (C,D) LKR-GFP (LKR protein trap), (E,F) *Drip* and (G,H) *ClC-a* *in situ* hybridisation. LKR, *Drip* and *ClC-a* expression is completely abolished in *tsh* knockdown SCs. Arrowheads in E,G. (**I-L**) *tsh* and *tio* regulate *ClC-a* expression redundantly in embryonic SCs. *ClC-a* expression (*in situ* hybridisation) in stage 17 embryos in wild type (I), *tsh* mutant (J), *tio* mutant (K) and *tsh tio* double mutant (L). *ClC-a* expression in embryonic SCs is unaffected in either *tsh* or *tio* mutants (arrowheads, I-K), but completely abolished in *tsh tio* double mutants (arrowhead indicates tubule position, L). Scale bars: 30 μm in A-H; 50 μm in I-L.

examined embryos mutant for the amorphic tsh^{8} allele. Interestingly, *ClC-a* expression in SCs is unaltered in tsh^{8} embryos (Fig. 4J). As *tio* is also expressed in SCs at this stage, it might contribute to *ClC-a* regulation in a redundant fashion with *tsh*. *ClC-a* is still expressed in SCs in amorphic tio^{S21} embryos (Fig. 4K); however, in *tsh tio* double mutants, *ClC-a* expression is completely abolished (Fig. 4L), demonstrating that *tsh* and *tio* have overlapping activities in the control of gene expression in embryonic SCs.

Regulation of cell shape

In wild-type animals, stellate and bar-shaped cells undergo a dramatic morphogenetic transformation during pupation from the cuboidal shape in larvae (Fig. 2I,K) to either a stellate-shaped (main segment; Fig. 2J,L; Fig. 5A,E) or bar-shaped (initial and transitional segments; Fig. 5B) morphology in adult tubules. Strikingly, these morphogenetic transformations do not occur in *tsh* knockdown; cells remain cuboidal both in the main and initial/transitional regions of adult tubules (Fig. 5C,D,F). Three-dimensional surface rendering reveals the full extent of shape differences between control and *tsh* knockdown SCs (Fig. 5E,F). As SCs provide the main transcellular passage for chloride ions and water, their large surface area is needed to support plasma membrane-resident chloride and water channels. *tsh* knockdown SCs have less than half the surface area of control SCs (Fig. 5G). This reduction in SC surface area could contribute to the poor physiological performance of *tsh* knockdown tubules (Fig. 3A).

Together, these data show that *tsh* contributes to cell differentiation by regulating multiple and diverse aspects of the cell phenotype, including cell morphology and the expression of terminal differentiation genes that have crucial physiological activities in SCs.

SC expression of *tio* rescues *tsh* knockdown

We asked whether SC expression of *tio* rescues any of the *tsh* knockdown phenotypes. We analysed the expression of *Drip*, *ClC-a* and *Lkr-GFP* in adult tubules of animals in which *tsh-RNAi* and *tio* had been driven with c724Gal4. *tio* is expressed strongly in SCs of these animals whereas Tsh is undetectable (Fig. 6A). The expression of *Lkr-GFP* and *Drip* is fully restored (Fig. 6B,C), but *ClC-a* is only weakly expressed in a subset of SCs. (Fig. 6D). However, SCs expressing *tio* show a clear stellate morphology (Fig. 6A′), indicating that the cell shape change can be driven by either *tio* or *tsh*. Adults that emerge are not bloated (Fig. 6E) and viability is partially rescued; 22% of *tio* rescued animals eclose compared with 12% of *tsh* knockdown (Fig. 6F).

These results show that although *tio* is not required for SC differentiation, it is sufficient for multiple aspects of SC maturation. However, full differentiation of SCs, including robust expression of *Clc-a*, and complete rescue of lethality (Fig. 6F) is specifically dependent on *tsh*.

Tsh acts through a transcription factor network to control cell differentiation

In the adult tubules of wild-type flies, *tsh* expression is restricted to SCs, whereas *cut* expression is restricted to PCs, suggesting mutual antagonism between these transcription factors (Fig. 7). To test whether Tsh represses *cut* expression in SCs, we examined Cut expression in *tsh*-knockdown tubules. Although *cut* is not expressed in wild-type SCs (Fig. 7A,B), its expression is ectopically induced to a level found in PCs after *tsh* knockdown (Fig. 7C). Thus, one function of Tsh is to repress *cut* expression in SCs. Furthermore, ectopic expression of Tsh in PCs (*CtB-Gal4 >UAS-tsh*, which induces a mosaic of *tsh*-expressing PCs) results in loss of Cut in cells expressing *tsh* (Fig. 7D), suggesting that Tsh represses *cut* expression. As *tsh* and *tio* act redundantly in the SCs of embryonic tubules, we used the same driver to express *tio* in PCs. Tio is also able to repress *cut*, and the degree of repression is proportional to the level of Tio induced (Fig. 7E).

We next asked whether Cut normally represses *tsh* expression in PCs. In embryos mutant for *cut*, SCs are not recruited to the developing tubules (Campbell et al., 2009) and morphogenesis is defective so that PCs form a blister associated with the hindgut (Hatton-Ellis et al., 2007). These mispositioned PCs do not express *tsh* (Campbell et al., 2009); however, if we drive ectopic *cut* expression in SCs (*c724 >UAS-cut*) *tsh* is repressed (Fig. 7F). Thus, although the presence of Cut is sufficient to repress *tsh* expression in SCs, factors other than Cut prevent *tsh* expression in developing PCs. Together, these data establish a negative cross-regulatory network between *cut* and *tsh*, in which it is crucial to exclude the expression of *cut* in SCs and of *tsh* in PCs (Fig. 7K).

We asked whether the decisive role of Tsh in SC differentiation is mediated through its repression of *cut*. We therefore analysed whether PCs in *cut* mutants express SC differentiation genes and found that *ClC-a* is not expressed (compare Fig. 7G with Fig. 4I).

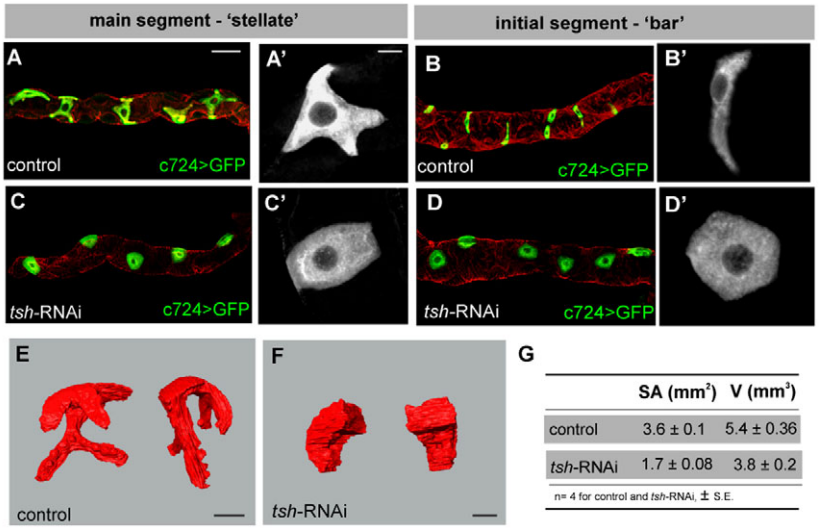

Fig. 5. *tsh* is required for SC morphology. (**A-D′**) Adult MpTs, SCs marked with c724>UAS-CD8GFP (green in A-D, white in A′-D′); tubules counterstained for actin (phalloidin, red). (A,B) Control tubules showing 'stellate'-shaped SCs in main segment (A,A′) and 'bar'-shaped cells in initial segment (B,B′). (C,D) *tsh* knockdown tubules have uncharacteristically round SCs in main (C,C′) and initial (D,D′) segments. (**E**,**F**) Three-dimensional reconstruction of control (E) and *tsh* knockdown (F) SCs shown from different angles. (**G**) Surface area and volume measurements for control (n=4) and *tsh* knockdown (n=4) SCs. (The reduction in volume accounts for only a 20% reduction in surface area in *tsh* knockdown SCs.) Scale bars: 30 μm in A-D; 10 μm in A′-D′,E,F.

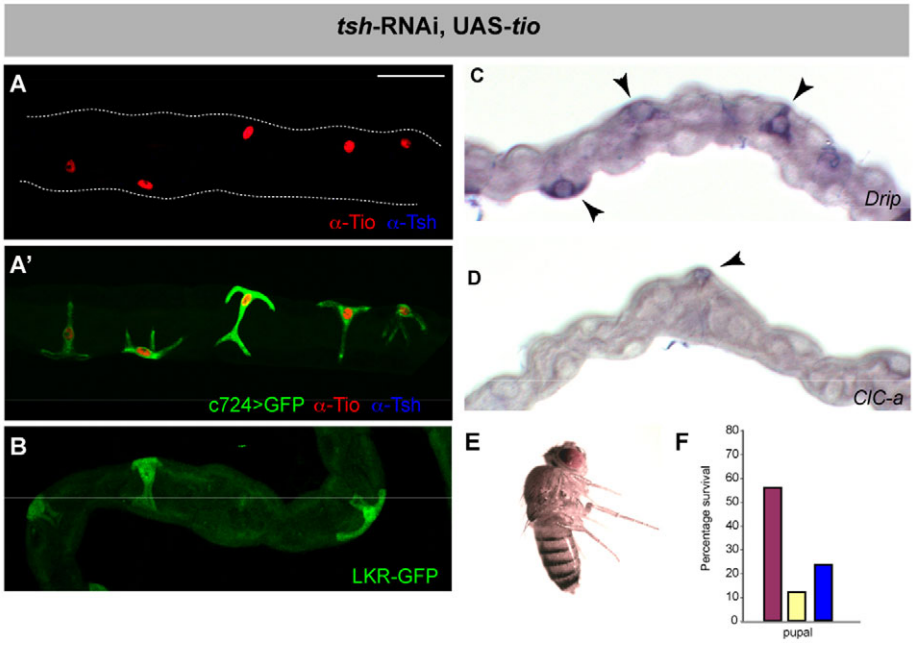

Fig. 6. *tio* is functionally equivalent to *tsh*. (**A**) Tio (red) and Tsh (blue) expression in SCs in c724>*tsh*-RNAi, UAS-*tio*, UAS-GFP adult MpT. Tio is expressed at high levels, whereas Tsh is undetectable. (**A′**) SCs morphology (c724>GFP, green) is rescued by Tio (red) in the absence of Tsh (blue). (B-F) Tio rescues SC gene expression, fluid homeostasis and lethality in the absence of Tsh. (**B-D**) Adult MpTs from c724>*tsh*-RNAi, UAS-*tio* animals LKR (B, LKR protein trap, green), and *Drip* (C) and ClC-a (D) *in situ* hybridisation. Arrowheads indicate SCs. (**E**) Adult c724>*tsh*-RNAi, UAS-*tio* do not exhibit fluid a homeostasis phenotype. (**F**) Survival rates of control (purple), knockdown (yellow) and c724>*tsh*-RNAi, UAS-*tio* (blue) expressed as percentage of adult hatching from 600, 900 and 324 embryos (four replicates carried out for *tio* rescue). Tio partly rescues the lethality associated with *tsh* knockdown. Scale bars: 30 μm in A-D.

We then asked whether ectopic *tsh*, and the consequent repression of *cut*, is sufficient to induce SC differentiation in PCs. In some cases, PC shape is transformed by ectopic *tsh* expression, leading to a more bar-shaped morphology (Fig. 7H,I) but we found no upregulation of genes normally expressed in SCs, such as LKR (Fig. 6J). These data suggest that although ectopic Tsh represses the expression of *cut* in PCs, loss of *cut* alone is not sufficient to induce SC differentiation.

Taken together, our data reveal that Tsh is a key factor in SC differentiation, acting at multiple levels that include the repression of *cut* (and thereby PC differentiation) and, independently, the induction of SC gene expression and morphology (Fig. 7K).

Conservation of *tsh* gene function

Morphologically distinct Type I and II MpT cells are widespread in insects (reviewed by Dow, 2012), suggesting that the segregation of physiological activities between different cell types is an ancient and conserved feature. To determine whether *tio*/*tsh* is expressed in Type II cells in other insect species, we chose the beetle *Tribolium castaneum* as a coleopteran [in which the *tio*/*tsh* orthologue is expressed in embryonic tubules (Shippy et al., 2008)] and the cricket *Gryllus bimaculatus* as an orthopteran representative. These species are distantly related to *Drosophila melanogaster* (a dipteran), sharing a common ancestor ~280 (beetle) and 360 (cricket) million years ago. Using the *Drosophila* Tio antibody, we probed the pattern of expression in adult tubules and found that the *tio*/*tsh* orthologue is expressed in the tubules of both *Tribolium* and *Gryllus* in a subset of cells with smaller nuclei than their neighbours and spaced in the same way as SCs in *Drosophila* tubules (Fig. 8A,B). These results reveal the presence of two cell subtypes in *Tribolium* and *Gryllus* tubules, and suggest that the differentiation of one of them (putative Type II cells) is under the control of *tio*/*tsh*. Together, our data imply that the presence of physiologically distinctive Type II cells and the control of their differentiation by the *tio*/*tsh* gene family are ancestral features of insect MpTs.

We have already shown that one of the vertebrate orthologues of the *tio*/*tsh* genes, *Tshz3*, is expressed in the ureteric mesenchyme around the ureteric duct of embryonic mouse kidney, where it is required for the differentiation of smooth muscle (SM) cells (Caubit et al., 2008). At the onset of the myogenic programme [embryonic day (E) 14.5], *Tshz3* is required *in vivo* for the expression of myocardin (*Myocd*), which enhances transcription of genes coding for smooth muscle cell contractile proteins [e.g. Smooth muscle actin alpha (SMAA) (Caubit et al., 2008)]. To characterise further the role of *Tshz3* in ureteric mesenchyme cell differentiation, we performed microarray expression profiling experiments by directly comparing samples of wild-type and *Tshz3*$^{-/-}$ mutant ureters at E14.5. To identify transcripts downregulated in the SM compartment of *Tshz3* mutant ureters at the onset of the myogenic programme, transcripts were ranked according to their *P*-value and we selected those with a *P*-value lower or equal to that of *Smaa*. The data filtering resulted in a list of 676 genes, representing 4.6% of 14,579 validated transcripts. The selected genes were tabulated in a descending order of the fold-change values. Among the 20 most downregulated genes are *Myocd* and several genes induced during smooth muscle differentiation [*Cnn1*, *Myh11*, *Actg2*, *Acta2* (*Sma-alpha*), Transgelin (*Sm22-alpha*)], indicating that this approach identifies a set of *Tshz3* target genes in the SM layer of the ureter (supplementary material Table S1). This set included the Aquaporin water conductance channel (AQP1) (supplementary material Table S1). As an independent experimental validation of the microarray analysis, we assessed the expression of AQP1 expression by immunofluorescence in E18.5 ureters in heterozygous control and *Tshz3* mutant mice. In wild-type or control ureters, AQP1 is expressed in the stromal layer, smooth muscle layer and outer mesenchymal layers (Fig. 8C,E). However, AQP1 expression in the smooth muscle layer, where *Tshz3* activity is known to be required for tissue differentiation (Caubit et al., 2008), is significantly reduced in *Tshz3* mutants compared with heterozygous controls (Fig. 8D,F). Thus, the regulatory activity of *Tshz3* in the mouse kidney shows parallels with the activity of *tsh* in insect MpTs in regulating specialised renal cell differentiation.

DISCUSSION

Together our results reveal a decisive role for *teashirt* in the differentiation of a physiologically distinctive cell type in the

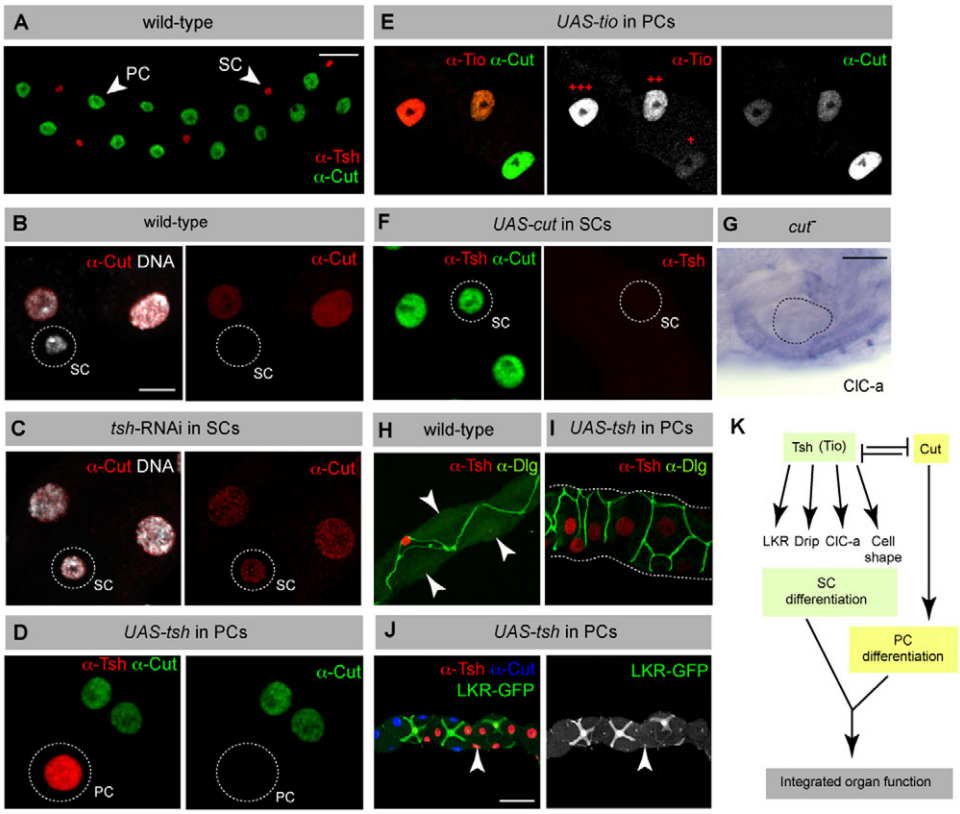

Fig. 7. The *tsh* gene network in SCs. (**A**) Wild-type adult tubule showing mutually exclusive expression of Cut (green) in PCs (large nuclei) and Tsh (red) in SCs (small nuclei). (**B**,**C**) Adult tubules stained for Cut (red) and DNA (white). In wild type (B), Cut is expressed in PCs (large nuclei) but not in SCs (small nucleus, circled). In *tsh* knockdown (C), Cut expression is ectopically induced in SCs (small nucleus, circled). (**D**) Adult tubule with induced ectopic expression of *tsh* in PCs (CtB>UAS-*tsh* results in mosaic *tsh* expression in PCs) stained for Cut (green) and Tsh (red). Ectopic Tsh in PCs (circled) leads to repression of Cut. (**E**) Adult tubule with ectopic expression of *tio* in PCs (CtB>UAS-*tio* results in mosaic and variable levels of *tio* expression in PCs) stained for Cut (green, white in individual channels) and Tio (red, white in individual channels). Ectopic *tio* expression in PCs leads to repression of Cut in a dose-dependent manner; high (+++), medium (++) and low (+) levels of Tio are indicated. (**F**) Adult tubule with ectopic expression of *cut* in SCs (c724>UAS-*cut*). Ectopic Cut expression leads to repression of Tsh in SCs (circled). (**G**) *ClC-a in situ* hybridisation in a *cut* mutant embryo. *ClC-a* is not ectopically expressed in PCs in the absence of Cut. The blister-shaped MpTs are outlined. (**H**,**I**) Adult MpTs stained for Disc-large (Dlg, green) to reveal cell shape and Tsh (red). Tsh-expressing PCs are transformed to a bar-shaped morphology (I) compared with control PCs (arrowheads, H). (**J**) Adult tubule with ectopic expression of *tsh* in PCs (CtB>UAS-*tsh* results in mosaic *tsh* expression in PCs) stained for Cut (blue), Tsh (red) and LKR-GFP (green, white in single channel image). LKR expression is not induced in Tsh-expressing PCs. (**K**) Schematic drawing of the gene network controlling PC and SC differentiation. Scale bars: 30 μm in A,H,I; 10 μm in B-F; 50 μm in G,J.

secretory region of the MpTs. *tsh* activity is required in Type II cells for the expression of genes that are key to their function, including chloride conductance (*ClC-a*), water conductance (*Drip*) and diuretic ligand sensitivity (*Lkr*). In addition, the eponymous cell shape changes that occur during pupation are abolished in the absence of *tsh*; SCs remain cuboidal, failing to extend arms around their PC neighbours to produce their stellate/bar shapes. Collectively, these defects in SC differentiation lead to a substantial reduction in viability, which we suggest is caused by defective excretion, as animals become bloated with fluid and the tubules fail to respond to diuretic stimuli, producing only very low levels of secreted primary urine.

Despite this prominent role for *tsh* in SC differentiation, it is clear that the emergence of Type II cells in the evolution of renal tubules was not dependent on the gene duplication that gave rise to *tsh*. Many insects with Type II cells, such as *Calliphora* (Berridge and Oschman, 1969), *Periplaneta* (Wall et al., 1975), *Carausius* (Taylor, 1971) and *Aedes* (O'Connor and Beyenbach, 2001), have only one *tio*/*tsh* family member. Furthermore, these cells have, in some cases, been shown to develop a stellate morphology in adult tubules. The function of Type II cells is not well understood in many species (see Taylor, 1971; Wessing et al., 1999), but in the mosquitoes *Aedes* and *Anopheles*, Type II cells show functional parallels with *Drosophila* SCs (reviewed by Beyenbach et al., 2010). Thus, aspects of the SC phenotype can develop and differentiate without the duplicated *tsh* gene. Our demonstration that the *tio*/*tsh* gene is expressed in a regularly spaced subset of tubule cells with small nuclei in both *Tribolium* and *Gryllus* suggests an evolutionarily conserved function for *tsh*-family members in Type II cell differentiation. We propose that the ancestral insect MpT contained two physiologically distinct cell types, where the differentiation of cells conducting anions and water was regulated by a Tio/Tsh-like transcription factor. We suggest that this state has been maintained in the tubules of most insects today, but in *Drosophila*, where a recent duplication has given rise to two paralogous genes, *tsh* has taken a predominant role. It will be interesting to determine whether the single *tio*/*tsh* gene is expressed in the MpTs of a wider range of insects, whether the pattern of expression correlates with the differentiation of SC-like characteristics, and whether gene knockdown results in

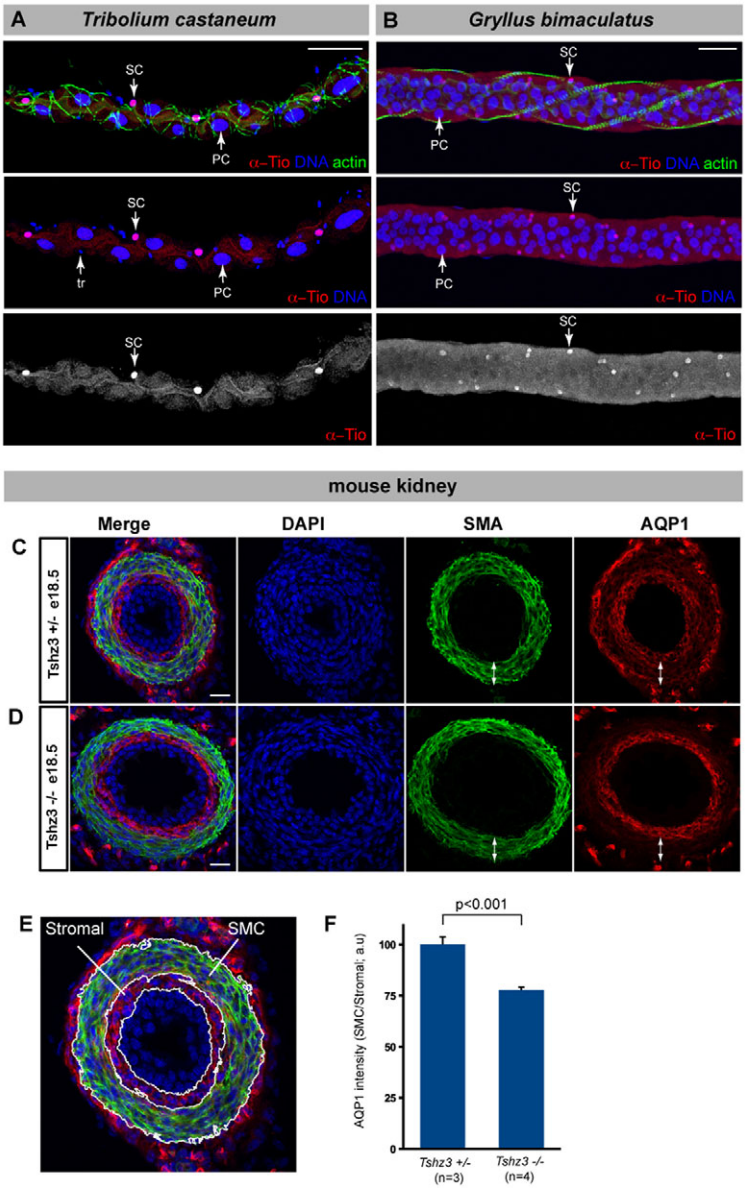

Fig. 8. Conservation of Tsh function. (**A**,**B**) MpTs from adult beetle (*Tribolium castaneum*) and cricket (*Gryllus bimaculatus*) stained with an antibody against *D.m*. Tio (red, white in single channel), DNA (blue) and actin (phalloidin, green). Tio marks a subset of MpTs cells with small nuclei interspersed with cells with larger nuclei. [In A, cells with the smallest nuclei (tr) correspond to tracheal cells.] (**C-E**) Cross-section through E18.5 mouse ureter stained for DAPI (blue), smooth muscle actin (SMA, green) and aquaporin 1 (AQP1, red), in sibling control (C) or Tshz3 homozygote (D). Double-headed arrows indicate smooth muscle layer. AQP1 expression in the smooth muscle layer is reduced in *Tshz3*$^{-/-}$ ureters. (E) Stromal and smooth muscle layer (SMC) are indicated in an enlarged image from C. (**F**) Quantification of AQP1 expression in the SMC by fluorescence intensity (expression in SMC was normalised relative to expression in the stromal layer). Both the wild-type and mutant ureters were sectioned distal to the ureteropelvic junction because of the severe hydroureter phenotype in the mutant ureter (Caubit et al., 2008). Scale bars: 50 μm in A,B; 25 μm in C,D.

defective Type II cell differentiation and organ physiology in these species.

Tsh acts as a transcriptional repressor in fly embryonic tissues (Alexandre et al., 1996; Andrew et al., 1994; de Zulueta et al., 1994; Fasano et al., 1991; Robertson et al., 2004; Röder et al., 1992) and in transfected mammalian cells (Waltzer et al., 2001). Correspondingly, we show that Tsh shuts down the expression of *cut* in SCs. Indeed, the expression of *cut* in neighbouring PCs depends on the exclusion of Tsh. In a reciprocal relationship, ectopic Cut represses *tsh* expression in SCs. Under normal conditions, this negative-feedback loop establishes two cell populations (Fig. 6A), with *cut*-expressing Type I cells and *tsh*-expressing Type II cells. Tio can also repress *cut* when ectopically expressed in PCs (Fig. 6E), indicating an ancestral repressive function for Tio/Tsh. We suggest that a genetic network centred around *cut* and *tio*/*tsh* leading to Type I and II cell differentiation is an ancient and widespread feature of insect MpT development.

However, neither transcription factor alone is sufficient for cell fate. *cut* acts together with *Krüppel* in wild-type PC differentiation (Hatton-Ellis et al., 2007) and the induction of *cut* in SCs does not transform them into PCs. Similarly, although ectopic Tsh in PCs represses *cut* expression and alters their shape, it does not produce transformation into the SC or bar-shaped cell architecture or the induction of SC-specific gene expression. Aspects of SC fate are controlled by factors other than *tsh* or *tio*; in *tio tsh* mutant embryos, cells integrate into the tubule epithelium (Campbell et al., 2010; Denholm et al., 2003) but simply fail to differentiate. Additionally, although all Type II cells express Tsh-driven *Drip*, *Lkr* and *ClC-a* (unpublished data), bar-shaped cells adopt different cell shapes and vary in their patterns of gene expression [such as c649-Gal4 in bar cells but not SCs (Sözen et al., 1997)]. These data indicate that additional regulators differentiate between bar and SCs. One candidate, Homothorax, is expressed exclusively in initial and transitional segments (unpublished data) (Kurant et al., 1998; Wang et al., 2004) and is known to act in concert with Tsh to pattern the developing adult eye, wing and leg (Azpiazu and Morata, 2000; Bessa et al., 2002; Casares and Mann, 2000).

In both mouse and possibly human kidney development *tsh*-family genes underlie the differentiation of ureteral smooth muscle (Caubit et al., 2008). Thus, in both vertebrate and *Drosophila*

nephrogenesis, these genes act to direct the differentiation of recruited mesenchymal cells that contribute, albeit with different functions, to the physiological competence of the mature organ.

Here, we show that, like *Drosophila* Tsh, mouse Tshz3 regulates the expression of a key differentiation gene, an aquaporin channel, in a specific subset of renal cells. The kidney phenotype of *Tshz3* mutant mice resembles congenital pelvi-ureteric junction obstruction, a common human kidney malformation (Caubit et al., 2008; Ek et al., 2007; Gunn et al., 1995; Ismaili et al., 2006), suggesting that *Tshz3* or its targets may contribute to the human disorder. Furthermore, Tsh-family members regulate cell differentiation in multiple contexts during vertebrate development and have roles in several human diseases (Feenstra et al., 2011; Jenkins et al., 2010; Schick et al., 2011; Yamamoto et al., 2011). Further analysis of Tsh and its target genes in *Drosophila* MpTs may identify effectors of physiological differentiation that are relevant to vertebrate nephrogenesis and organogenesis, as well as potential candidate human disease genes.

Acknowledgements
We thank members of the Skaer laboratory for helpful discussions, Felix Evers for advice on 3D cell reconstruction, Simon Maddrell for help with the *in vitro* secretion assay, Christine Vola and Dr E. Martin for RNA sample preparation, Kathrin Saar and Sabine Schmidt for performing gene expression experiments, and Herbert Schulz for statistical analysis of the microarray and helpful discussion. We are grateful to Justin Kumar, Fernando Casares, Matt Benton and Berthold Hedwig for insect stocks and to Stephen Cohen for antibodies.

Funding
Research was supported by Centre National de la Recherche Scientifique (CNRS), Association Française contre les Myopathies (AFM) [12545, 13013] and Agence Nationale de la Recherche (ANR) [ANR-09-GENO-027-01 to L.F.]; by The Wellcome Trust [094879/A/10/Z to H.S.]; by Alliance: Franco-British Partnership Programme (H.S. and L.F.); and by Kidney Research UK [PDF1/2010 to B.D.]. Deposited in PMC for immediate release.

Competing interests statement
The authors declare no competing financial interests.

Supplementary material
Supplementary material available online at
http://dev.biologists.org/lookup/suppl/doi:10.1242/dev.088989/-/DC1

References

Al-Anzi, B., Armand, E., Nagamei, P., Olszewski, M., Sapin, V., Waters, C., Zinn, K., Wyman, R. J. and Benzer, S. (2010). The leucokinin pathway and its neurons regulate meal size in Drosophila. *Curr. Biol.* **20**, 969-978.
Alexandre, E., Graba, Y., Fasano, L., Gallet, A., Perrin, L., De Zulueta, P., Pradel, J., Kerridge, S. and Jacq, B. (1996). The Drosophila teashirt homeotic protein is a DNA-binding protein and modulo, a HOM-C regulated modifier of variegation, is a likely candidate for being a direct target gene. *Mech. Dev.* **59**, 191-204.
Andrew, D. J., Horner, M. A., Petitt, M. G., Smolik, S. M. and Scott, M. P. (1994). Setting limits on homeotic gene function: restraint of Sex combs reduced activity by teashirt and other homeotic genes. *EMBO J.* **13**, 1132-1144.
Azpiazu, N. and Morata, G. (2000). Function and regulation of homothorax in the wing imaginal disc of Drosophila. *Development* **127**, 2685-2693.
Berridge, M. J. and Oschman, J. L. (1969). A structural basis for fluid secretion by malpighian tubules. *Tissue Cell* **1**, 247-272.
Bessa, J. and Casares, F. (2005). Restricted teashirt expression confers eye-specific responsiveness to Dpp and Wg signals during eye specification in Drosophila. *Development* **132**, 5011-5020.
Bessa, J., Gebelein, B., Pichaud, F., Casares, F. and Mann, R. S. (2002). Combinatorial control of Drosophila eye development by eyeless, homothorax, and teashirt. *Genes Dev.* **16**, 2415-2427.
Bessa, J., Carmona, L. and Casares, F. (2009). Zinc-finger paralogues tsh and tio are functionally equivalent during imaginal development in Drosophila and maintain their expression levels through auto- and cross-negative feedback loops. *Dev. Dyn.* **238**, 19-28.
Beyenbach, K. W., Skaer, H. and Dow, J. A. (2010). The developmental, molecular, and transport biology of Malpighian tubules. *Annu. Rev. Entomol.* **55**, 351-374.
Cabrero, P., Radford, J. C., Broderick, K. E., Costes, L., Veenstra, J. A., Spana, E. P., Davies, S. A. and Dow, J. A. (2002). The Dh gene of Drosophila melanogaster encodes a diuretic peptide that acts through cyclic AMP. *J. Exp. Biol.* **205**, 3799-3807.
Campbell, K., Knust, E. and Skaer, H. (2009). Crumbs stabilises epithelial polarity during tissue remodelling. *J. Cell Sci.* **122**, 2604-2612.
Campbell, K., Casanova, J. and Skaer, H. (2010). Mesenchymal-to-epithelial transition of intercalating cells in Drosophila renal tubules depends on polarity cues from epithelial neighbours. *Mech. Dev.* **127**, 345-357.
Casares, F. and Mann, R. S. (2000). A dual role for homothorax in inhibiting wing blade development and specifying proximal wing identities in Drosophila. *Development* **127**, 1499-1508.
Caubit, X., Lye, C. M., Martin, E., Coré, N., Long, D. A., Vola, C., Jenkins, D., Garratt, A. N., Skaer, H., Woolf, A. S. et al. (2008). Teashirt 3 is necessary for ureteral smooth muscle differentiation downstream of SHH and BMP4. *Development* **135**, 3301-3310.
Caubit, X., Thoby-Brisson, M., Voituron, N., Filippi, P., Bévengut, M., Faralli, H., Zanella, S., Fortin, G., Hilaire, G. and Fasano, L. (2010). Teashirt 3 regulates development of neurons involved in both respiratory rhythm and airflow control. *J. Neurosci.* **30**, 9465-9476.
Clark, A. G., Eisen, M. B., Smith, D. R., Bergman, C. M., Oliver, B., Markow, T. A., Kaufman, T. C., Kellis, M., Gelbart, W., Iyer, V. N. et al. (2007). Evolution of genes and genomes on the Drosophila phylogeny. *Nature* **450**, 203-218.
Coast, G. M., Webster, S. G., Schegg, K. M., Tobe, S. S. and Schooley, D. A. (2001). The Drosophila melanogaster homologue of an insect calcitonin-like diuretic peptide stimulates V-ATPase activity in fruit fly Malpighian tubules. *J. Exp. Biol.* **204**, 1795-1804.
Datta, R. R., Lurye, J. M. and Kumar, J. P. (2009). Restriction of ectopic eye formation by Drosophila teashirt and tiptop to the developing antenna. *Dev. Dyn.* **238**, 2202-2210.
Datta, R. R., Cruickshank, T. and Kumar, J. P. (2011a). Differential selection within the Drosophila retinal determination network and evidence for functional divergence between paralog pairs. *Evol. Dev.* **13**, 58-71.
Datta, R. R., Weasner, B. P. and Kumar, J. P. (2011b). A dissection of the teashirt and tiptop genes reveals a novel mechanism for regulating transcription factor activity. *Dev. Biol.* **360**, 391-402.
de Zulueta, P., Alexandre, E., Jacq, B. and Kerridge, S. (1994). Homeotic complex and teashirt genes co-operate to establish trunk segmental identities in Drosophila. *Development* **120**, 2287-2296.
Denholm, B., Sudarsan, V., Pasalodos-Sanchez, S., Artero, R., Lawrence, P., Maddrell, S., Baylies, M. and Skaer, H. (2003). Dual origin of the renal tubules in Drosophila: mesodermal cells integrate and polarize to establish secretory function. *Curr. Biol.* **13**, 1052-1057.
Denholm, B., Brown, S., Ray, R. P., Ruiz-Gómez, M., Skaer, H. and Hombría, J. C. (2005). crossveinless-c is a RhoGAP required for actin reorganisation during morphogenesis. *Development* **132**, 2389-2400.
Dow, J. A. (2012). The versatile stellate cell - more than just a space-filler. *J. Insect Physiol.* **58**, 467-472.
Dow, J. A. T. and Davies, S. A. (2001). The *Drosophila melanogaster* Malpighian Tubule. *Adv. Insect Physiol.* **28**, 1-83.
Dow, J. T. and Davies, S. A. (2003). Integrative physiology and functional genomics of epithelial function in a genetic model organism. *Physiol. Rev.* **83**, 687-729.
Dow, J. A., Maddrell, S. H., Görtz, A., Skaer, N. J., Brogan, S. and Kaiser, K. (1994). The malpighian tubules of Drosophila melanogaster: a novel phenotype for studies of fluid secretion and its control. *J. Exp. Biol.* **197**, 421-428.
Ek, S., Lidefeldt, K. J. and Varricio, L. (2007). Fetal hydronephrosis; prevalence, natural history and postnatal consequences in an unselected population. *Acta Obstet. Gynecol. Scand.* **86**, 1463-1466.
Erickson, T., Pillay, L. M. and Waskiewicz, A. J. (2011). Zebrafish Tshz3b negatively regulates Hox function in the developing hindbrain. *Genesis* **49**, 725-742.
Erkner, A., Gallet, A., Angelats, C., Fasano, L. and Kerridge, S. (1999). The role of Teashirt in proximal leg development in Drosophila: ectopic Teashirt expression reveals different cell behaviours in ventral and dorsal domains. *Dev. Biol.* **215**, 221-232.
Faralli, H., Martin, E., Coré, N., Liu, Q. C., Filippi, P., Dilworth, F. J., Caubit, X. and Fasano, L. (2011). Teashirt-3, a novel regulator of muscle differentiation, associates with BRG1-associated factor 57 (BAF57) to inhibit myogenin gene expression. *J. Biol. Chem.* **286**, 23498-23510.
Fasano, L., Röder, L., Coré, N., Alexandre, E., Vola, C., Jacq, B. and Kerridge, S. (1991). The gene teashirt is required for the development of Drosophila embryonic trunk segments and encodes a protein with widely spaced zinc finger motifs. *Cell* **64**, 63-79.
Feenstra, I., Vissers, L. E., Pennings, R. J., Nillessen, W., Pfundt, R., Kunst, H. P., Admiraal, R. J., Veltman, J. A., van Ravenswaaij-Arts, C. M., Brunner, H. G. et al. (2011). Disruption of teashirt zinc finger homeobox 1 is associated with congenital aural atresia in humans. *Am. J. Hum. Genet.* **89**, 813-819.

Georgias, C., Wasser, M. and Hinz, U. (1997). A basic-helix-loop-helix protein expressed in precursors of Drosophila longitudinal visceral muscles. *Mech. Dev.* **69**, 115-124.
Gunn, T. R., Mora, J. D. and Pease, P. (1995). Antenatal diagnosis of urinary tract abnormalities by ultrasonography after 28 weeks' gestation: incidence and outcome. *Am. J. Obstet. Gynecol.* **172**, 479-486.
Hatton-Ellis, E., Ainsworth, C., Sushama, Y., Wan, S., VijayRaghavan, K. and Skaer, H. (2007). Genetic regulation of patterned tubular branching in Drosophila. *Proc. Natl. Acad. Sci. USA* **104**, 169-174.
Henderson, K. D., Isaac, D. D. and Andrew, D. J. (1999). Cell fate specification in the Drosophila salivary gland: the integration of homeotic gene function with the DPP signaling cascade. *Dev. Biol.* **205**, 10-21.
Herke, S. W., Serio, N. V. and Rogers, B. T. (2005). Functional analyses of tiptop and antennapedia in the embryonic development of Oncopeltus fasciatus suggests an evolutionary pathway from ground state to insect legs. *Development* **132**, 27-34.
Ismaili, K., Hall, M., Piepsz, A., Wissing, K. M., Collier, F., Schulman, C. and Avni, F. E. (2006). Primary vesicoureteral reflux detected in neonates with a history of fetal renal pelvis dilatation: a prospective clinical and imaging study. *J. Pediatr.* **148**, 222-227.
Jenkins, D., Caubit, X., Dimovski, A., Matevska, N., Lye, C. M., Cabuk, F., Gucev, Z., Tasic, V., Fasano, L. and Woolf, A. S. (2010). Analysis of TSHZ2 and TSHZ3 genes in congenital pelvi-ureteric junction obstruction. *Nephrol. Dial. Transplant.* **25**, 54-60.
Johnson, E. C., Shafer, O. T., Trigg, J. S., Park, J., Schooley, D. A., Dow, J. A. and Taghert, P. H. (2005). A novel diuretic hormone receptor in Drosophila: evidence for conservation of CGRP signaling. *J. Exp. Biol.* **208**, 1239-1246.
Kaufmann, N., Mathai, J. C., Hill, W. G., Dow, J. A., Zeidel, M. L. and Brodsky, J. L. (2005). Developmental expression and biophysical characterization of a Drosophila melanogaster aquaporin. *Am. J. Physiol. Cell Physiol.* **289**, C397-C407.
Kean, L., Cazenave, W., Costes, L., Broderick, K. E., Graham, S., Pollock, V. P., Davies, S. A., Veenstra, J. A. and Dow, J. A. (2002). Two nitridergic peptides are encoded by the gene capability in Drosophila melanogaster. *Am. J. Physiol. Regul. Integr. Comp. Physiol.* **282**, R1297-R1307.
Koebernick, K., Kashef, J., Pieler, T. and Wedlich, D. (2006). Xenopus Teashirt1 regulates posterior identity in brain and cranial neural crest. *Dev. Biol.* **298**, 312-326.
Kurant, E., Pai, C. Y., Sharf, R., Halachmi, N., Sun, Y. H. and Salzberg, A. (1998). Dorsotonals/homothorax, the Drosophila homologue of meis1, interacts with extradenticle in patterning of the embryonic PNS. *Development* **125**, 1037-1048.
Laugier, E., Yang, Z., Fasano, L., Kerridge, S. and Vola, C. (2005). A critical role of teashirt for patterning the ventral epidermis is masked by ectopic expression of tiptop, a paralog of teashirt in Drosophila. *Dev. Biol.* **283**, 446-458.
Maddrell, S. H. P. (1981). The functional design of the insect excretory system. *J. Exp. Biol.* **90**, 1-15.
Maddrell, S. H., Herman, W. S., Mooney, R. L. and Overton, J. A. (1991). 5-Hydroxytryptamine: a second diuretic hormone in Rhodnius prolixus. *J. Exp. Biol.* **156**, 557-566.
Manfroid, I., Caubit, X., Kerridge, S. and Fasano, L. (2004). Three putative murine Teashirt orthologues specify trunk structures in Drosophila in the same way as the Drosophila teashirt gene. *Development* **131**, 1065-1073.
Mathies, L. D., Kerridge, S. and Scott, M. P. (1994). Role of the teashirt gene in Drosophila midgut morphogenesis: secreted proteins mediate the action of homeotic genes. *Development* **120**, 2799-2809.
O'Connor, K. R. and Beyenbach, K. W. (2001). Chloride channels in apical membrane patches of stellate cells of Malpighian tubules of Aedes aegypti. *J. Exp. Biol.* **204**, 367-378.
O'Donnell, M. J., Rheault, M. R., Davies, S. A., Rosay, P., Harvey, B. J., Maddrell, S. H., Kaiser, K. and Dow, J. A. (1998). Hormonally controlled chloride movement across Drosophila tubules is via ion channels in stellate cells. *Am. J. Physiol.* **274**, R1039-R1049.
Quiñones-Coello, A. T., Petrella, L. N., Ayers, K., Melillo, A., Mazzalupo, S., Hudson, A. M., Wang, S., Castiblanco, C., Buszczak, M., Hoskins, R. A. and Cooley, L. (2007). Exploring strategies for protein trapping in Drosophila. *Genetics* **175**, 1089-1104.
Radford, J. C., Davies, S. A. and Dow, J. A. (2002). Systematic G-protein-coupled receptor analysis in Drosophila melanogaster identifies a leucokinin receptor with novel roles. *J. Biol. Chem.* **277**, 38810-38817.
Ramsay, J. A. (1954). Active transport of water by the Malpighian tubules of the stick insect, *Dixippus morosus* (Orthoptera, Phasmidae). *J. Exp. Biol.* **31**, 104-113.
Robertson, L. K., Bowling, D. B., Mahaffey, J. P., Imiolczyk, B. and Mahaffey, J. W. (2004). An interactive network of zinc-finger proteins contributes to regionalization of the Drosophila embryo and establishes the domains of HOM-C protein function. *Development* **131**, 2781-2789.
Röder, L., Vola, C. and Kerridge, S. (1992). The role of the teashirt gene in trunk segmental identity in Drosophila. *Development* **115**, 1017-1033.
Santos, J. S., Fonseca, N. A., Vieira, C. P., Vieira, J. and Casares, F. (2010). Phylogeny of the teashirt-related zinc finger (tshz) gene family and analysis of the developmental expression of tshz2 and tshz3b in the zebrafish. *Dev. Dyn.* **239**, 1010-1018.
Schick, B., Wemmert, S., Willnecker, V., Dlugaiczyk, J., Nicolai, P., Siwiec, H., Thiel, C. T., Rauch, A. and Wendler, O. (2011). Genome-wide copy number profiling using a 100K SNP array reveals novel disease-related genes BORIS and TSHZ1 in juvenile angiofibroma. *Int. J. Oncol.* **39**, 1143-1151.
Shippy, T. D., Tomoyasu, Y., Nie, W., Brown, S. J. and Denell, R. E. (2008). Do teashirt family genes specify trunk identity? Insights from the single tiptop/teashirt homolog of Tribolium castaneum. *Dev. Genes Evol.* **218**, 141-152.
Singh, A., Kango-Singh, M. and Sun, Y. H. (2002). Eye suppression, a novel function of teashirt, requires Wingless signaling. *Development* **129**, 4271-4280.
Singh, A., Kango-Singh, M., Choi, K. W. and Sun, Y. H. (2004). Dorso-ventral asymmetric functions of teashirt in Drosophila eye development depend on spatial cues provided by early DV patterning genes. *Mech. Dev.* **121**, 365-370.
Soanes, K. H. and Bell, J. B. (1999). Rediscovery and further characterization of the aeroplane (ae) wing posture mutation in Drosophila melanogaster. *Genome* **42**, 403-411.
Soanes, K. H., MacKay, J. O., Core, N., Heslip, T., Kerridge, S. and Bell, J. B. (2001). Identification of a regulatory allele of teashirt (tsh) in Drosophila melanogaster that affects wing hinge development. An adult-specific tsh enhancer in Drosophila. *Mech. Dev.* **105**, 145-151.
Sözen, M. A., Armstrong, J. D., Yang, M., Kaiser, K. and Dow, J. A. (1997). Functional domains are specified to single-cell resolution in a Drosophila epithelium. *Proc. Natl. Acad. Sci. USA* **94**, 5207-5212.
Sudarsan, V., Pasalodos-Sanchez, S., Wan, S., Gampel, A. and Skaer, H. (2002). A genetic hierarchy establishes mitogenic signalling and mitotic competence in the renal tubules of Drosophila. *Development* **129**, 935-944.
Sun, Y. H., Tsai, C. J., Green, M. M., Chao, J. L., Yu, C. T., Jaw, T. J., Yeh, J. Y. and Bolshakov, V. N. (1995). White as a reporter gene to detect transcriptional silencers specifying position-specific gene expression during Drosophila melanogaster eye development. *Genetics* **141**, 1075-1086.
Tang, C. Y. and Sun, Y. H. (2002). Use of mini-white as a reporter gene to screen for GAL4 insertions with spatially restricted expression pattern in the developing eye in drosophila. *Genesis* **34**, 39-45.
Taylor, H. H. (1971). The fine structure of the type 2 cells in the Malpighian tubules of the stick insect, Carausius morosus. *Z. Zellforsch. Mikrosk. Anat.* **122**, 411-424.
Terhzaz, S., O'Connell, F. C., Pollock, V. P., Kean, L., Davies, S. A., Veenstra, J. A. and Dow, J. A. (1999). Isolation and characterization of a leucokinin-like peptide of Drosophila melanogaster. *J. Exp. Biol.* **202**, 3667-3676.
Wall, B. J., Oschman, J. L. and Schmidt, B. A. (1975). Morphology and function of Malpighian tubules and associated structures in the cockroach, Periplaneta americana. *J. Morphol.* **146**, 265-306.
Waltzer, L., Vandel, L. and Bienz, M. (2001). Teashirt is required for transcriptional repression mediated by high Wingless levels. *EMBO J.* **20**, 137-145.
Wang, J., Kean, L., Yang, J., Allan, A. K., Davies, S. A., Herzyk, P. and Dow, J. A. (2004). Function-informed transcriptome analysis of Drosophila renal tubule. *Genome Biol.* **5**, R69.
Wessing, A. and Eichelberg, D. (1978). *Malpighian Tubules, Rectal Papillae and Excretion.* London: Academic Press.
Wessing, A., Zierold, K. and Polenz, A. (1999). Stellate cells in the Malpighian tubules of Drosophila hydei and D. melanogaster larvae (Insecta, Diptera). *Zoomorphology* **119**, 63-71.
Wu, J. and Cohen, S. M. (2000). Proximal distal axis formation in the Drosophila leg: distinct functions of teashirt and homothorax in the proximal leg. *Mech. Dev.* **94**, 47-56.
Wu, J. and Cohen, S. M. (2002). Repression of Teashirt marks the initiation of wing development. *Development* **129**, 2411-2418.
Yamamoto, M., Cid, E., Bru, S. and Yamamoto, F. (2011). Rare and frequent promoter methylation, respectively, of TSHZ2 and 3 genes that are both downregulated in expression in breast and prostate cancers. *PLoS ONE* **6**, e17149.

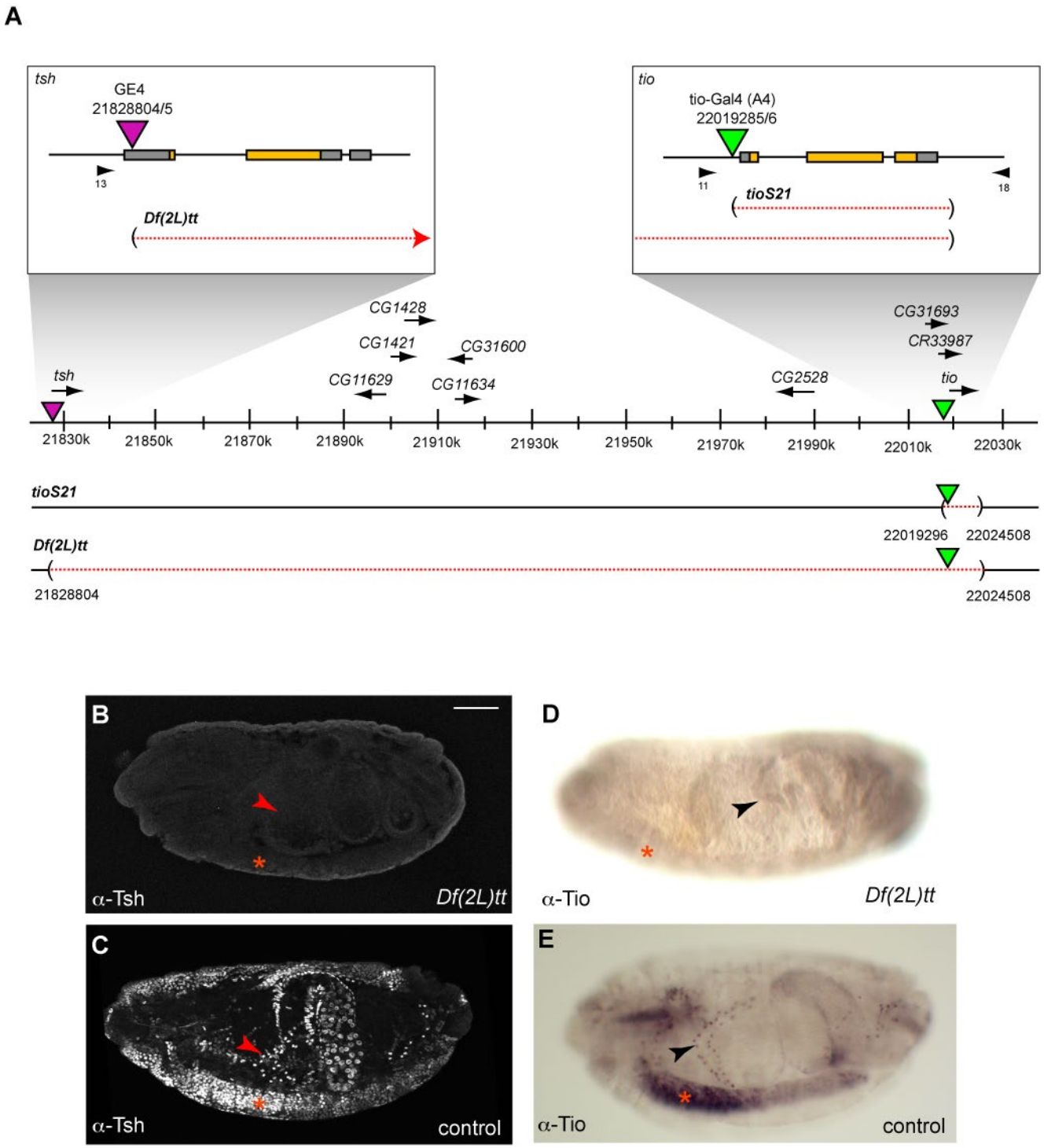

Fig. S1. Molecular mapping of the *tsh-tio* and *tio* deficiency lines. (**A**) The *tsh-tio* genomic locus spans cytological positions 40A5 to 40D3 and is ~200 kb in length. The centromere is on the right. More detailed views of the *tsh* and *tio* loci are illustrated in the upper boxes and show intron-exon structure, coding sequence (yellow) and extent of the genomic deficiencies (red dashed lines between brackets). There are seven predicted but uncharacterised protein-coding genes and one non-protein coding gene (*CR33987*) between *tsh* and *tio* (arrows). The P-element insertions used to generate the deficiencies are shown as triangles (*tsh*, purple and *tio*, green) and their genomic insertion points are given. The insertion in *tio* has been described previously by Tang and Sun (Tang and Sun, 2002) , where it is referred to as *tioA4*. The insert in *tsh* (*GE4*) was generated as part of this study. *tioS21* and *Df(2L)tt* are depicted below, with the extent of the genomic deficiency indicated by the broken red line between brackets. Primer sets 13+18 and 11+18 (arrowheads) were used to amplify across the deficiencies for sequencing. A region of the P-element remained after excision of *tio-Gal4(A4)* and is present in *tioS21* and *Df(2L)tt* deficiency lines. *tioS21* removes *tio* and part of the overlapping gene *CR33987*. *Df(2L)tt* removes all genes between and inclusive of *tsh* and *tio*. *tios21* is a protein null for Tio (data not shown). (**B-E**) *Df(2L)tt* is a protein null for Tsh and Tio. Tsh (B,C) and Tio (D,E) expression in *Df(2L)tt* (B,D) and sibling control (C,E) embryos. Arrowheads indicate anterior MpT and asterisk indicates staining in the central nervous system. Scale bars: 50 μm.

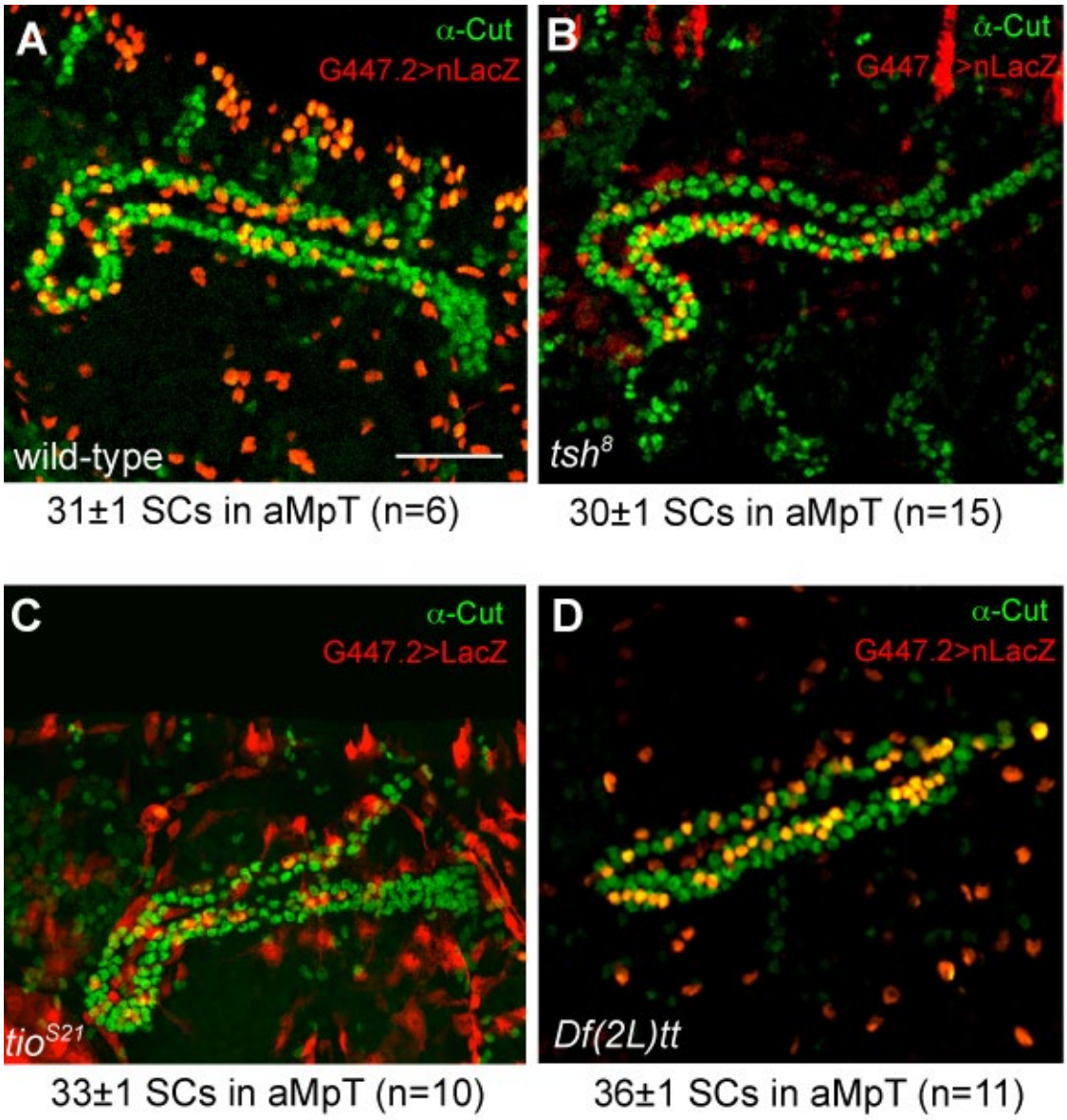

Fig. S2. Tsh and Tio show little or no morphological MpT defects in embryos. (A-D) Stage 16 embryonic MpTs stained for Cut (green) and the SC-marker G447.2>*lac*Z (red). SCs are present with approximately the normal number and normal spacing in *tsh* (**B**) and *tio* (**C**) single mutants and *tsh tio* double mutants (**D**), compared with wild-type (**A**). SC numbers for each genotype are given. Scale bars: 50 μm.

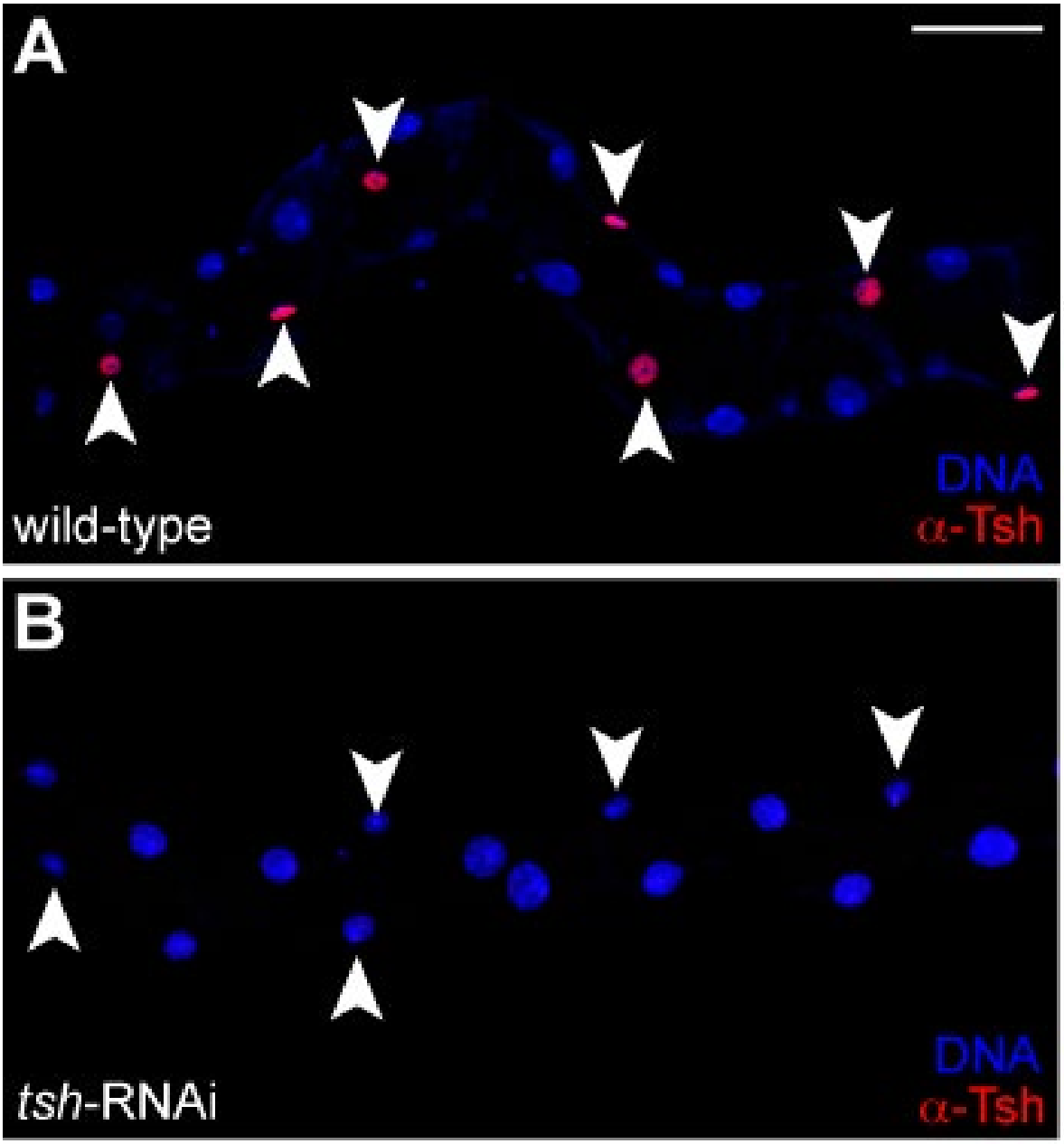

Fig. S3. Effective Tsh knockdown by RNAi. (A,B) Adult Malpighian tubules stained for Tsh (red) and DNA (blue). Arrowheads indicate SCs (identified by their small nuclear size compared to PCs). (**A**) Wild-type tubule, Tsh is expressed in all SCs. (**B**) *c724>UAS-tsh-RNAi*, Tsh expression is abolished in SCs after RNAi knockdown (a total of 38 *c724>UAS-tsh-RNAi* tubules were examined, corresponding to over 1000 SCs). Scale bars: 30 μm.

Table S1. The 20 most downregulated genes in E14.5 *Tshz3* mutant ureters

	Fold change (KO versus WT)	**Gene symbol**	**Gene title**
10583809	−2.953	Cnn1	calponin 1
10437885	−2.748	Myh11	myosin, heavy polypeptide 11, smooth muscle
10545707	−2.531	Actg2	actin, gamma 2, smooth muscle (Smaa)
10386996	−2.476	Myocd	myocardin
10579054	−2.160	4930467E23Rik	RIKEN cDNA 4930467E23 gene
10538459	−2.158	Aqp1	aquaporin 1
10528177	−2.129	Speer4e	spermatogenesis associated glutamate (E)-rich protein
10603232	−2.118	Gmcl1l	germ cell-less homolog 1 (Drosophila)-like
10467124	−2.114	Acta2	actin, alpha 2, smooth muscle
10350630	−2.081	Fam129a	family with sequence similarity 129, member A
10571601	−2.053	Pdlim3	PDZ and LIM domain 3
10577388	−2.007	4930467E23Rik	RIKEN cDNA 4930467E23 gene
10528183	−2.004	Speer4e	spermatogenesis associated glutamate (E)-rich protein
10345101	−1.895	Col9a1	collagen, type IX, alpha 1
10578045	−1.883	Nrg1	// neuregulin 1
10599673	−1.866	4930527E24Rik	RIKEN cDNA 4930527E24 gene
10485711	−1.843	Fibin	fin bud initiation factor homolog (zebrafish)

10603986	−1.825	RP23-110D11.1	Xlr-related, meiosis regulated Xmr
10566810	−1.818	Nrip3	nuclear receptor interacting protein 3
10593123	−1.787	Tagln	Transgelin (Sm22)

The 20 most downregulated genes in E14.5 Tshz3 mutant ureters. Shown are fold change mutant (KO)/wild-type ureters. Several downregulated genes in *Tshz3* mutant ureters are genes usually induced during smooth muscle differentiation [calponin, *Myh11*, *Actg2*, *Acta2* (*Sma-alpha*), transgelin (*Sm22-alpha*)]. The downregulation of *Aqp1* (−2.15) is superior to *Sma* (−2.11) and *Sm22* (−1.78), the expression regulation of which by *Tshz3* has been previously shown by immunohistochemistry (Caubit et al., 2008). Fold change = –1(experimental/reference). Values represent average over three independent experiments. The results were quantile normalised with respect to the probe GC content using the RMA algorithm (GC content adjustment, RMA background correction and mean probe set summarisation). Transcripts either not expressed or expressed at very low levels were removed by a maximum expression cutoff <100. This data filtering resulted in 173,540 of 234,872 probe sets and 22,495 meta-probe sets. After normalisation, the arrays were checked for outliers using the principal component analysis with a correlation dispersion matrix and normalised Eigenvector scaling. No outliers were detected. Microarray probe sets representing transcripts changed by twofold or more were further analyzed. This data filtering resulted in 14,579 listed genes. Differential expression of summarised gene level expression was calculated using the Partek two-way ANOVA statistic followed by false discovery rate (FDR) multiple testing correction. Resulting *P*-values and FDR values indicated the probability of differential expression in state (wild type/knockout) and stage (embryonic stages 14 and 16). 2240 transcript clusters with an ANOVA FDR<0.05 in one of the conditions (genotype, stage, genotype*stage interaction) were defined as the significant differentially expressed subset.